Bioinspired nano-ordered liquid membrane for precise molecular separation

Haozhen Dou
University of Waterloo
Mi Xu
Tianjin University
Baoyu Wang
Zhengzhou University of Technology
Zhen Zhang
University of Waterloo
Guobin Wen
University of Waterloo
Dan Luo
University of Waterloo
Feifei Peng
Tianjin University
Aiping Yu
University of Waterloo
Zhengyu Bai
Henan Normal University
Zhongyi Jiang
Tianjin University
Zhongwei Chen (zhwchen@uwaterloo.ca)
University of Waterloo https://orcid.org/0000-0003-3463-5509

Article

Keywords: bioinspired nano-ordered liquid membrane, ethylene/ethane separation, molecule separations

Posted Date: October 7th, 2020

DOI: https://doi.org/10.21203/rs.3.rs-87445/v1

Abstract

Cellular membranes provide ideal archetypes for molecule or ion separations with sub-angstrom scale precision, which are featured with both extremely high permeability and selectivity due to the well-defined membrane protein channels. However, the development of bioinspired membranes with artificial channels for sub-angstrom scale ethylene/ethane (0.416 nm / 0.443 nm) separation remains an uncharted territory and a significant challenge. Herein, a bioinspired nano-ordered liquid membrane is constructed by a facile ion/molecule self-assembly strategy for highly efficient ethylene/ethane separation, which mimics the structure of cellular membrane elegantly and possesses plenty of three-dimensional (3D) nanochannels. The elaborate regulation of non-covalent interactions by optimizing the ion/molecule compositions within membrane confers the nano-ordered liquid structure with interpenetrating and bi-continuous apolar domains and polar domains, which results in the formation of regular carrier wires and enormous 3D interconnected ethylene transport nanochannels. By virtue of these 3D nanochannels, the bioinspired nano-ordered liquid membrane manifests simultaneously super-high selectivity, excellent permeance and long-term stability, which exceeds previously reported ethylene/ethane separation membranes. This methodology in this work for construction of bioinspired membrane with tunable 3D nanochannels through ion/molecule self-assembly will enlighten the design and development of high-performance separation membranes for angstrom/sub-angstrom scale ion or molecule separations.

Introduction

Membrane separation is a well-established and forward-looking technology,[1, 2, 3] where novel materials, versatile architectures and fascinating applications spring up exuberantly.[4, 5, 6, 7] Membranes possess inherent attributes of high energy efficiency, good environmental safety, cost-effectiveness and small plant footprint, which exhibit grand potential for enormous separations in energy and environment fields.[8, 9, 10, 11] However, the implementation of membranes for angstrom/sub-angstrom scale precise ion or molecule separations such as ion sieving, chiral recognition and olefin/paraffin separation still remains a major global challenge,[12, 13, 14] and the corresponding high-performance membranes are urgently needed.[15, 16] Cellular membranes regulate the selective transport of sub-angstrom/angstrom scale ions or molecules with exceptional selectivity and superhigh transport rates, such as ions, water, gas and organic molecules for cell metabolism.[17] The combination of high permeability and selectivity is primarily attributed to the sophisticated membrane structure with a variety of specialized membrane proteins or aquaporins (AQPs) embedded in the phospholipid bilayer,[7, 18] which can be described by fluid mosaic model.[19] On the one hand, the lipid bilayer is a dynamic two-dimensional fluid, which renders the cellular membrane with elasticity and flexibility.[20] On the other hand, driven by intermolecular forces, bilayer-spanning helices are assembled into versatile membrane proteins with N- and C-termini heading towards the cytosol, and these specialized membrane proteins are featured with well-defined angstrom-scale channels and chemical functionality,[21, 22] which synergistically combine size, charge, van der Waals, and other specific binding interactions to achieve the selective and super-fast transport of target species.[23, 24]

For example, the AQP within cellular membrane exhibits a high permeability of 3×10^9 H_2O molecules per second per AQP subunit but completely excludes all ionic species;[25] the CO_2 permeability can reach up to 120000 molecules per second per AQP subunit;[26] the potassium permeation rate is ~ 10^8 ions/s with a super high potassium/ sodium ion selectivity of ~ 1000.[2]

The elegant structure and unprecedented performances of cellular membranes provide archetypes and grant germane inspirations for the design of highly efficient membranes for sub-angstrom/angstrom-scale ion or molecule separations.[27, 28] The integration of AQP within the matrix of polymer or graphene oxide membranes is the direct method to construct bioinspired membranes.[29, 30] However, the difficult manipulation of orientation and connectivity of AQPs, their intricate structure, high cost and low stability severely hinder further applications of AQP based membranes.[27] Recently, artificial channel-based bioinspired membranes that mimic the structures and functions of cellular membranes have emerged and are more appealing due to their easy fabrication and high stability, which can be divided into two categories based on their channel construction: unimolecular channel membrane and self-assembling channel membrane.[28] Unimolecular channel such as the carbon nanotube is generally inserted into lipid bilayers to construct bioinspired membranes for energy-efficient water purification due to the frictionless water flow in single-file chain.[31, 32] In contrast, the self-assembling channels are constructed from self-assembly of small building blocks by weak intermolecular forces such as hydrophobic interactions or hydrogen bonding,[33, 34] which offer advantages of chemical diversity, precise control of channel architecture and easy fabrication.[24, 27] However, most reported bioinspired membranes with artificial channel are small-membrane vesicles with diameter of ~200 nm, meanwhile the low-density channels often result in low separation performances.[35] Therefore, novel bioinspired membrane with plenty of transport channels as well as cost- and process-efficient membrane construction strategy are still highly needed yet challenging, particularly when considering the fabrication of scalable membranes for practical applications.

Ionic liquids are combinations of cations and anions, which can generate a variety of attractive interactions ranging from the weak forces (van der Waals, dispersion forces) to strong forces (hydrogen bonding and electrostatic interactions). [36, 37, 38] The diverse intermolecular forces and structural designability of ILs make them easily assemble into versatile nanostructures.[39, 40] Therefore, ILs are anticipated to be a novel and leading candidate for developing bioinspired membranes with transport nanochannels.[41, 42] Herein, we present, from inception to implementation, a family of bioinspired nano-ordered liquid membranes with excellent separation performance for ethylene/ethane (0.416 nm / 0.443 nm) separation,[43] which are constructed from ion/molecule self-assembly of protic salts (PSs, solid protic ionic liquids at room temperature), polyol and ethylene-transport carrier ($AgNO_3$), where the PSs imitate phospholipid molecules, and the combination of polyol and $AgNO_3$ carrier imitates carrier protein. The regulation of hydrogen bonding, electrostatic and amphiphilicity interactions by optimizing their compositions can confer the nano-ordered liquid structure with interpenetrating and continuous apolar domains and polar domains, which results in the formation of regular carrier wires and enormous

3D interconnected ethylene transport nanochannels. The plenty of nanochannels effectively reduce the distances for the transport and enable continuous and fast transport of ethylene molecules throughout nano-ordered liquid membranes. Moreover, the eutectics of PS and polyol make their mixture remain liquid state with fluidity and elasticity at room temperature, which contributes to facile scalable membrane fabrication by spin-coating. Ethylene/ethane separation is a typical example of sub-angstrom scale separations and has been recognized as one of the seven chemical separations to challenge the world as a consequence of extremely similar molecular size and huge global energy consumption for separation.[44, 45] The implementation of bioinspired nano-ordered liquid membrane for ethylene/ethane separation has the potential to create significant cost and environmental savings in relative to cryogenic distillation.[46, 47] The bioinspired nano-ordered liquid membrane manifests simultaneously super-high selectivity, excellent permeability and long-term stability, which exceeds the advanced ethylene/ethane separation membranes. This work opens up a novel and efficient avenue to worldwide challenging ethylene/ethane separation, and the methodology that manipulating directional distribution of silver ions to construct fast transport nanochannels will shed light on design advanced membrane materials in separations, catalyst and battery applications.[48, 49]

Results And Discussions

Membrane design and morphology characterization. The bioinspired nano-ordered liquid membranes are constructed from ion/molecule self-assembly strategy to imitate the structure of cellular membrane. For the structural design of bioinspired nano-ordered liquid membranes, $AgNO_3$ is chosen as the carrier because of its low cost, facile availability and excellent ability of transporting ethylene; PSs, as a subclass of ionic liquids, are chosen due to their same anion with carrier, useful protic acidic properties to stabilize silver carrier and their tunable intermolecular forces, especially amphiphilicity and electrostatic interactions; the natural and renewable polyols such as glycerol have conspicuous advantages of strong hydrogen-bond interactions and low material cost. A variety of PSs such as EAN, DEAN, TEAN, MIMN, CPAN and three typical polyols of EG, G and TEG are screened for the investigation of their structural effects on the self-assembly behaviors and corresponding separation performances of membranes (Figure S1). The physical property of as-selected PSs and their structural characterizations by ^1H NMR and FTIR spectra are shown in Table S1 and Figure S2-S3. A series of binary liquid eutectics of PSs and polyols, and ternary eutectics of PSs, polyols and silver salt carrier (also referred to as membrane liquid) are formed with nano-ordered structure due to strong interactions, which is verified by their low melting points (Table S2). The bioinspired liquid membranes are easily fabricated by spin-coating of as-designed nano-ordered membrane liquid onto a home-made PES support (Figure 1a and Figure S4), where nanopores of support (about 100 nm) and the suitable viscosity of membrane liquid confer facile accumulation of membrane liquid on the support surface to form stable selective separation layer. Moreover, the chemical synthesis of membrane liquid is also highlighted by taking EAN (PS) and G (polyol) as an example (Figure $1a_1$), which comprises two steps of synthesizing EAN by proton transfer reaction and mixing as-prepared EAN, $AgNO_3$ and G. The amphiphilicity, hydrogen bonding and electrostatic attractions endow the resultant membranes with inhomogeneous and nano-ordered liquid

structures, where molecular and ionic clusters are found within the complex and ordered hydrogen-bond networks. The amphiphilicity interactions of the PS cations make themselves aggregate together into apolar nano-regions. The hydrogen bonding and electrostatic attractions lead to the formation of polar nano-domains, which are composed of with polyol, silver cation and NO_3^- anions. Therefore, the self-assembled nano-ordered liquid membrane share the distinct structural similarity with cellular membrane (Figure 1b), where the self-assembly of PSs mimics the lipid bilayer (Figure $1b_1$), the self-assembly of glycerol embedded within carrier mimics the carrier protein (Figure $1b_2$), being expected to possess incomparable gas permeability and selectivity like cellular membrane.

The distinctive feature of bioinspired liquid membrane is the precise manipulation of carrier distribution, including the continuity, the aggregation and the corresponding activity. Optimally, the arrangement of the nano-ordered polar and apolar domains can be tailored by the content of PS, polyol or their molar ratios, which results in the formation of regular carrier wires and enormous 3D interconnected ethylene transport nanochannels (Figure 1d). The continuous carrier distribution and high carrier activity contribute to the ultrafast and selective ethylene transport, which afford the combined high ethylene permeability and super-high ethylene/ethane selectivity (Figure $1d_1$). In contrast, the traditional polymer or liquid membranes generally possesses discrete and disordered carrier distribution with low carrier activity (Figure 1e), suffering from the very sluggish transport of ethylene molecules (Figure $1e_1$). Moreover, the impertinent combination of Ps and polyol or their molar ratio will lead to the lousily carrier aggregation with poor carrier activity, resulting in unattractive ethylene/ethane selectivity (Figure 1c). The morphology of bioinspired nano-ordered liquid membranes is investigated by SEM (Figure 1f-1k). The home-made PES support has relatively uniform pore sizes of ~100 nm and hierarchical cross-section structure with a relative dense top layer and a finger-like macroporous sublayer (Figure 1f and 1g). After spin-coating for several times, the support is completely covered by membrane liquid and a selective separation layer of nano-ordered liquid with ~5 μm is clearly obtained (Figure 1h and 1i). Figure 1j and 1k show the photos of pristine support and as-designed bioinspired nano-ordered liquid membrane, which further confirm the successful membrane fabrication. The facile membrane manufacturing by spin-coating making them more attractive for large scale industrial applications. Finally, the bioinspired nano-ordered liquid membranes exhibit desirable thermal stability as revealed by TG curves (Figure S5)

Characterizations of non-covalent intermolecular forces. The intermolecular forces driving self-assembly of nano-ordered liquid structure are investigated by the DSC, ^{1}H NMR, ATR-FTIR and FT-Raman spectra (Figure 2), especially for the electrostatic and strong hydrogen-bonding interactions.[50] The eutectic property among PSs, polyols and carrier is confirmed by the low melting points, which vary from -68 to -91.5 ^oC and are significantly manipulated by the combination of PS and polyol and the corresponding molar ratio. The incorporation of $AgNO_3$ within binary eutectics of PS and polyol further increases melting points slightly (Figure 2a). The eutectic property indicates the collapse of crystal structure of PS and the weakened electrostatic interactions between the cation and anion by mixing. Meanwhile, eutectics make membrane remain liquid state and possess similar dynamic fluidity with cellular membranes, which renders the membrane with elasticity and flexibility, contributing to the defect-free

membranes. Other physical properties of the membrane liquid, such as density, ion conductivity and the viscosity, are also collected in Table S2. As shown in Figure 2b, the NH_3^+ and OH chemical shifts in pure [EAN] locate at 7.832 and 4.590 ppm. Upon mixing with G, the chemical shift of NH_3^+ moves to up-filed gradually with the molar ratios of EAN to G changing from 1:1 to 1:3, which manifests that the electrostatic interactions and double ionic hydrogen bonds between cation and anion in PSs are weakened by the intercalation of PS by G. Concomitantly, the chemical shift of OH in G moves to up-fields by mixing PS, suggesting the hydrogen bond interactions among G molecules are broken and new hydrogen bond interactions between [G] and [EAN] are built. As seen from Figure 2c, the FTIR spectra of PS-polyol binary eutectic exhibits the characteristic bands of [EAN] and [G], and the hydrogen bonds existing as N-H···O and O-H···O have been confirmed by the broad peaks between 3600 and 3200 cm^{-1}. The deformation vibrations of NH_3^+ and stretching vibrations of NO_3^- are found to be blue-shifts with the molar ratio of EAN to G decreasing from 1:1 to 1:3, which further indicates the collapse of long-range ordered structure of the PS.

The stretching modes of the OH in PS-polyol eutectic exhibit blue-shifts, implying that the hydrogen bond interactions of G-PS cation and G- PS anion are weaker than that of G-G. The ^1H NMR and FTIR spectra of EG and TEG based binary eutectics exhibit similar behaviors with that of G-based binary eutectics (Figure S6-S7). However, the extent of shifts varies with different polyol and molar ratios, which indicates the tunable nano-ordered structures of bioinspired liquid membranes with different polyols. Subsequently, the incorporation of silver salt carrier to form membrane liquid (ternary eutectics), where the intermolecular forces between carrier and PS or polyol are also probed by ATR-FTIR spectra (Figure 3d). Upon introduction of silver salt, the OH stretching vibrations of polyols exhibit different red shifts for G, EG and TEG based membrane liquids, which indicated the diverse coordinative interactions between silver cation and polyols.[51, 52] Meantime, the red-shifts of NO_3^- stretching vibrations are also observed, hinting the possible formation of hydrogen bonds between NO_3^- of silver salt and polyols. The G based membrane liquid exhibits stronger red shifts than EG and TEG based membrane liquids, which implies the stronger coordinative and hydrogen bond interactions. As elucidated in Figure 2e-2g, the deconvoluted FT-Raman spectra further gain insight of the ionic species in bioinspired nano-ordered liquid membranes with different PS/polyol molar ratios. Note that the NO_3^- stretching bands of free ions, ion pairs, and ion aggregates are located at 1034, 1040, and 1045 cm^{-1}, respectively. For the PS/polyol molar ratio of 1:2, the ion aggregates are the dominant ionic constituents. For the PS/polyol molar ratio of 1:1, the content of ion aggregates decreases, while ion pairs and free ions increase. When the molar ratio of is 1:3, the free ions and ion pairs predominate. FT-Raman clearly indicates the PS/polyol molar ratios also govern the nano-ordered structure of bioinspired liquid membranes.

Visualization of nano-ordered membrane structure. The visualization of nano-ordered structure of bioinspired liquid membranes and the resultant carrier distributions are conducted by molecular dynamics simulations and small- and wide-angle X-ray scattering (SWAXS) at nanoscale level. The highlighted snapshot of bulk structure of bioinspired liquid membrane (EAN: glycerol = 1:1) in

equilibrated simulation box reveals a bicontinuous nano-ordered structure analogous to the morphology of cellular membrane (Figure 3a), where the EAN cations (yellow) are assembled into apolar nanodomains to imitate lipid molecular layer, while the EAN anions (red), silver salt and G (blue) are assembled into polar nanodomains to act as carrier protein. The snapshot of bulk structure of bioinspired liquid membrane are shown in Figure 3b, and the isolated snapshots of cations, anions and glycerol further discern the self-assembled nano-ordered structure clearly (Figure 3c, 3e and 3f).

Cation alkyl chains are solvophobically associated together into apolar domains due to amphiphilic interactions, where carbon atoms orient towards each other with the ammonium groups facing away (figure 3c). The NO_3^- anions and G molecules are assembled together to form polar nanodomains due to strong electrostatic and hydrogen-bonding interactions, where NO_3^- anions are aligned upon the corresponding positions of cation charge group, and the G molecules or their clusters locate around charge groups of EAN (Figure 3e and 3f). Nearly all the silver salts confine themselves within polar nanodomains because of strong coordinative and hydrogen bond interactions. The periodic and well-defined nano-order structure of bioinspired liquid membrane are further confimed by radial distribution functions of ion-ion or ion-molecular, gij(r). The cation-cation and anion-anion peaks further suggest their aggregations within apolar and polar nanodomains, respectively. The stronger G-G peak in relative to G-Cation and G-anion indicates the presence of clusters of G molecules due to stronger hydrogen bonding interactions among G molecules (Figure 3j). The radial distribution functions of atom-atom highlight the strong electrostatic interactions between the cation and anion are retained in membrane liquid, where the NH_3^+ tends to approach the NO_3^- at closer distances (Figure 3k). The radial distribution functions of silver-anion, silver-G and silver-cations suggest the silver cations are encircled by NO_3^- anions and solvated by G molecules due to electrostatic and hydrogen-bonding interactions, respectively (Fig. S8). The coordination number quantificationally describe the intensity of hydrogen bonds (Table S3), which follows the order: G-G > G-cation > G-anion. The nano-ordered structure of bioinspired liquid membranes with EAN/G molar ratio of 1:2 is shown in Figure 3d and the isolated snapshots of cations, anions and glycerol are shown in Figure S9, which suggests the continuous polar domains but discrete apolar domains with the increase of G molecules. The polar domains occupy a larger fraction of the stimulated box, which results in the severe compression of apolar domains. The distributions of silver cations within bioinspired liquid membranes with EAN/G molar ratios of 1:1 and 1:2 are shown in Figure 3g and Figure 3h. The bicontinuous and interpenetrating networks of polar and apolar within bioinspired liquid membranes (1:1) lead to the continuous and uniform carrier distribution to create the regular carrier networks (highlighted in Figure 3i). Therefore, enormous 3D interconnected ethylene transport nanochannels are formed and contribute to the ultrafast and selective ethylene transport, which afford the excellent separation performances of bioinspired liquid membranes (1:1). In contrast, the distribution of silver cations within bioinspired liquid membranes (1:2) can be divided into two situations: uniform but discrete distribution and severe aggregation of most silver cations, which lead to poor carrier activity, resulting in poor separation performances of bioinspired liquid membranes (1:2). It can be inferred that the apolar domains will be further diluted by G clusters with the G molecules increasing continuously. The silver cations within bioinspired liquid membranes (1:3) are uniformly but discretely dispersed in the polar

domains and solvated by G molecules, which render the membrane with moderate separation performances.

Moreover, the SWAXS further reveals the intermediate-range order of bioinspired liquid membrane. For the bioinspired liquid membrane (Ag/[EAN:G=1:1]), the peak at low q (< 1 $Å^{-1}$) can be assigned as a correlation peak arising from segregation of the alkyl chains into apolar domains, which clearly indicates the intermediate range nano-ordered structure (Fig. 3l). Correlation distance between the ammonium head groups can be approximated from the q values of the peaks through the use of Bragg's Law of d = 2π/q, which is about 10 Å. The other correlation peak located at ~1.7 $Å^{-1}$ has been attributed to the distance between alkyl chains. However, no peak is observed for [EAN: G] at low q (< 1 $Å^{-1}$), which suggests the small disordered cluster structure. This difference further confirms the vital role of carrier for the construction of nano-ordered structure, which is indicative by the compact alkyl chain configuration.

Evaluation of separation performances. The separation performances of bioinspired nano-ordered liquid membranes are evaluated by carrying out equimolar ethylene/ethane mixture separation on our home-made facility (Figure S10), and the operational procedure can be found in Supporting Information. The effects of the PS, Polyol, and their molar ratio on the membrane separation performances are investigated systematically, which gains insight of the membrane structure-performance relationships. As shown in Figure 4a, the PSs greatly affect the gas permeability. The effect of PSs on the ethylene permeability follows the sequence of MIMN > EAN > DEAN > TEAN > CAPN, which suggests ethylene permeability can be improved by skillful selection of PSs. As expected, the order of ethane permeability is in good agreement with the viscosities of membrane liquid due to that its permeation is mainly dependent on Fick diffusion (Figure S11). With the introduction of more hydroxyl groups into PSs, the decrease of ethane permeability is quicker than that of ethylene, which is probably attributed to the compact nano-ordered membrane structure induced by the presence of more hydroxyl groups. Therefore, the gas selectivity sharply increases with the more hydroxyl groups into PSs and reaches up to 265 for [TEAN] derived bioinspired nano-ordered liquid membrane, which is the highest ethylene/ethane selectivity ever reported. As shown in Figure 4b and Figure S12, the ethylene permeability of the membranes based on three different polyols follows the order of EG > G > TEG, while the ethylene/ethane selectivity is as follows: G > EG >TEG, which is arisen from by the different carrier activity within the different polyol derived polar domains. The silver cations surrounded by G molecules are more active due to stronger coordinative and hydrogen bond interactions. The PS/polyol molar ratios significantly determine carrier distribution within bioinspired nano-ordered liquid membranes, resulting in diverse separation performances. As expected by the above molecular dynamics simulation, the ethylene permeability obtains maximum at the molar ratio of 1:1, median at the molar ratio of 1:3 and minimum at molar ratio of 1:2 (Figure 4c). In contrast, the ethane permeability possessed maximum at the molar ratio of 1:2, which is almost 1~2 orders of magnitude higher than values obtained at the molar ratios of 1:1 and 1:3. The unusual ethane permeability at the molar ratio of 1:2 is ascribed to lousily carrier aggregation. Therefore, ethylene/ethane selectivity decreases initially and then increases with the PS/polyol molar ratio of changing from 1:1 to 1:3, obtaining a maximum at the molar ratio of 1:1, which

originates from enormous 3D interconnected ethylene transport nanochannels (Figure 4d). As seen from Figure S13, the ethylene permeability increases gradually with the silver salt content increasing from 0 to 5 mol/L, and the gas selectivity initially increases slightly and then increased sharply, varying from 3.4 to 226 for EAN derived membrane, which is attributed to more continuous and available carrier for ethylene transport. Moreover, an initial parameter optimization is conducted to promote the process efficiency, including transmembrane pressure, operating temperature, the feed ratio of ethylene/ethane and the flow rate of sweep gas (Figure S14), where the decrease of the transmembrane pressure favors separation selectivity but goes against the gas permeability, while the decrease of operating temperature has a completely opposite effect on the gas selectivity and permeability, the permeability decreases but selectivity increases. Moreover, the increase of the flow rate of sweep gas and the feed ratio not only improves the gas selectivity but also enhances the gas permeability. Fortunately, bioinspired nano-ordered liquid membranes present long-term stability during continuous operating, which clearly show a tempting prospect for commercial success. Finally, the excellent separation performances of as-designed membranes are highlighted by in comparison with those of traditional and advanced ethylene/ethane separation membranes (Figure 4f and Figure S15), and the highly competitive permeability and superhigh slectivity make them more promising than previously reported polymeric membranes, carbon molecular sieve membranes (CMS), mixed matrix membranes (MMMs), carrier-facilitated transport membranes (FTMs), IL and deep eutectic solvent (DES) based liquid membranes and metal organic framework membranes (MOF).

Discussion

In summary, we have developed a series of bioinspired nano-ordered liquid membranes constructed from ion/molecule self-assembly of PS, polyol and ethylene-transport carrier ($AgNO_3$), which mimic the structure of cellular membranes to achieve high-performance ethylene/ethane separation. The eutectics of PS and polyol make membrane remain liquid state and possess similar dynamic fluidity with cellular membranes, contributing to the facile scalable fabrication of defect-free membranes by spin-coating. The intermolecular forces are investigated by various spectroscopic characterizations and the visualization of nano-ordered membrane structure is conducted by molecular dynamics simulations. The amphiphilicity, hydrogen bonding and electrostatic attractions within membranes drive the self-assembly of ion/molecule into nano-ordered liquid structure with interpenetrating and continuous apolar domains and polar domains, which can precisely manipulate of the carrier distribution such as the continuity, aggregation and activity. By optimizing the PS and polyol and their compositions, the regular carrier wires with continuous and uniform carrier distribution are obtained, resulting in the formation of enormous 3D interconnected ethylene transport nanochannels. The plenty of nanochannels effectively reduce the mass transport distances as well as enable continuous and fast transport of ethylene molecules throughout nano-ordered liquid membranes. The elucidation of stucture-performance relationship further confirms the 3D nanochannels and suggests that ethylene permeability and gas selectivity can be greatly improved by rational selection the PSs, polyol, and their molar ratios. Moreover, the bioinspired nano-ordered liquid membranes exhibit good long-term stability. Therefore, the excellent separation

performances and good long-term stability may herald this new class of bioinspired membranes as promising alternatives to the existing separation technology, and the pioneering exploration to construct fast transport nanochannels by ion/molecule self-assembly will shed light on the development of channel-based membranes, highly conductive electrolytes and controlled metal-distributed catalysts for energy and environmental applications.

Methods

Preparation of bioinspired nano-ordered liquid membranes. The nano-ordered membrane liquids were prepared by mixing PS, polyol and silver salt at the PS/polyol molar ratios of 1:1, 1:2 and 1:3 with magnetic agitation at 60 ^{o}C until the clear and colourless liquids were formed. The membrane liquids were then dried under vacuum to remove excess moisture and their water contents were determined by Karl-Fischer titration method to be less than 1000 ppm. Then the bioinspired nano-ordered liquid membranes were obatined by spin-coating of above as-synthesized membrane liquids on home-made PES support using spin coater (KW-4S, SETCAS Electronics Co. Ltd. Beijing, China), which fellowed a similar procedure as our previous reports.[42] In order to obtain stable selective separation layer, the coating procedure was repeated several times (about 3~5).

Characterization. The densities were determined at 25 °C with a Mettler-Toledo DE40 density meter. The viscosities were measured by a Brookfield DV1 digital viscometer. The ionic conductivity measurements were carried out by using DDSJ-318 Conductivity Meters. The melting points were acquired with differential scanning calorimetry (DSC, 200F3, NETZSCH Co). The thermal gravimetric analysis (TGA) was performed by a Netzsch TG 209 thermal gravimetric analyser. The ^{1}H NMR spectra were recorded on the VARIA INOVA 400MHz spectrometer using DMSO-d6 as solvent. The Fourier transform infrared spectra (FTIR) were recorded on a Nicolet MAGNA-IR 560 spectroscopy with a resolution of 4 cm^{-1} in the range of 4000-400 cm^{-1}. Fourier transform Raman spectra (FT-Raman) were carried out by a Raman spectrometer (Bruker RFS 100). The microscopic morphology of membranes was obtained by the field emission scanning electron microscope (SEM, FESEM, Nova Nanosem 430, FEI Co., USA). Synchronous wide-angle and small-angle X-ray scattering was conducted at beamline 1W2A of the Beijing Synchrotron Radiation Facility, China.

MD simulations. The nanostructure of bioinspired nano-ordered liquid membrane was investigated by molecular dynamics simulations using large scale atomic/molecular massively parallel simulator (LAMMPS) package. In the MD simulations, an initial configuration containing 600 PAN ion pairs, 600 glycerinum molecules, and 300 $AgNO_3$ molecules was randomly distributed within a large cubic initial simulation box. The initial configuration was then equilibrated at T=400 K with a constant NPT simulation for 1 ns. This system was then re-equilibrated at T = 800 K under constant NVT conditions for 1 ns. The final configuration of 800 K was then cooled down sequentially to 400 K, at intervals of 100 K. For each temperature interval, the system was equilibrated for 500 ps, and finally for 1 ns at 400 K. The

trajectory data was saved each 0.1 ps for other 100 ps under NVT ensemble. The integration time step was 1.0 fs. Periodic boundary conditions are applied to the models.

separation performance test. Mixed-gas permeation experiments were performed as our previous report and the set-up was shown in Supporting Information.[53] The gas permeation experiments were performed at desired conditions. Three parallel experiments were carried out to obtain the stable values. For mixed gas experiments, the permeability(P_i) and C_2H_4/C_2H_6 selectivity ($S_{i,j}$) could be calculated by thefollowing equations.

$$P_i = \mathrm{J}_i \frac{\delta}{\Delta P_i} \quad (1)$$

$$S_{i,j} = \frac{P_{m,i}}{P_{m,j}} \quad (2)$$

Where P_i is the gas permeability of component i (Barrer), J_i is the permeation flux of component i ($cm^3/(cm^2 \cdot S)$); δ is the membrane thickness (cm); and ΔP_i is the pressure difference between the feed and permeate side (cmHg).

Declarations

Data availability

The authors declare that all data supporting the findings of this study are available within the paper and its supplementary information files. The data that support the findings of this study are available from the corresponding author upon reasonable request.

Acknowledgements

We acknowledge the financial support by Natural Sciences and Engineering Research Council of Canada (NSERC), University of Waterloo, Waterloo Institute for Nanotechnology, National Natural Science Foundation of China (21838008). Thank National Supercomputing Center in Shenzhen for computational facilities.

Author contributions

H. Dou, M. Xu and Z. Jiang, Z. Chen devised the idea. H. Dou, M. Xu and F. Peng conducted the experiments. H. Dou, B. Wang and Z. Zhang cowrote the manuscript. G. Wen and D. Luo conducted MD simulation. and made efforts on writing the manuscript. A. Yu, Z. Bai, Z. Jiang, Z. Chen gave valuable advices along the work. All authors discussed the results.

Competing interests

The authors declare no competing interests.

References

1. Koros WJ, Zhang C. Materials for next-generation molecularly selective synthetic membranes. Nat Mater 2017, 16(3): 289–297.
2. Park HB, Kamcev J, Robeson LM, Elimelech M, Freeman BD. Maximizing the right stuff: The trade-off between membrane permeability and selectivity. *Science* 2017, **356**(6343): eaab0530.
3. Yang Y, Yang X, Liang L, Gao Y, Cheng H, Li X, *et al.* Large-area graphene-nanomesh/carbon-nanotube hybrid membranes for ionic and molecular nanofiltration. *Science* 2019, **364**(6445): 1057–1062.
4. Liu G, Chernikova V, Liu Y, Zhang K, Belmabkhout Y, Shekhah O, *et al.* Mixed matrix formulations with MOF molecular sieving for key energy-intensive separations. *Nat Mater* 2018, **17**(3): 283–289.
5. Ali Z, Ghanem BS, Wang Y, Pacheco F, Ogieglo W, Vovusha H, *et al.* Finely Tuned Submicroporous Thin-Film Molecular Sieve Membranes for Highly Efficient Fluid Separations. *Adv Mater* 2020, **32**(22): 2001132.
6. Dey K, Kunjattu H S, Chahande AM, Banerjee R. Nanoparticle Size-Fractionation through Self-Standing Porous Covalent Organic Framework Films. *Angewandte Chemie International Edition* 2020, **59**(3): 1161–1165.
7. Dou H, Xu M, Jiang B, Wen G, Zhao L, Wang B, *et al.* Bioinspired Graphene Oxide Membranes with Dual Transport Mechanisms for Precise Molecular Separation. *Advanced Functional Materials* 2019, **29**(50): 1905229.
8. Liang B, Wang H, Shi X, Shen B, He X, Ghazi ZA, *et al.* Microporous membranes comprising conjugated polymers with rigid backbones enable ultrafast organic-solvent nanofiltration. *Nature Chemistry* 2018, **10**(9): 961–967.
9. Cai Y, Chen D, Li N, Xu Q, Li H, He J, *et al.* A Self-Cleaning Heterostructured Membrane for Efficient Oil-in-Water Emulsion Separation with Stable Flux. *Adv Mater* 2020, **32**(25): 2001265.
10. Nie L, Goh K, Wang Y, Lee J, Huang Y, Karahan HE, *et al.* Realizing small-flake graphene oxide membranes for ultrafast size-dependent organic solvent nanofiltration. *Science Advances* 2020, **6**(17): eaaz9184.
11. Jiang Z, Karan S, Livingston AG. Water Transport through Ultrathin Polyamide Nanofilms Used for Reverse Osmosis. *Adv Mater* 2018, **30**(15): 1705973.
12. Chen L, Shi G, Shen J, Peng B, Zhang B, Wang Y, *et al.* Ion sieving in graphene oxide membranes via cationic control of interlayer spacing. *Nature* 2017, **550**: 380.
13. Liang Y, Zhu Y, Liu C, Lee K-R, Hung W-S, Wang Z, *et al.* Polyamide nanofiltration membrane with highly uniform sub-nanometre pores for sub-1 Å precision separation. *Nature Communications* 2020, **11**(1): 2015.
14. Wang Y, Wu N, Wang Y, Ma H, Zhang J, Xu L, *et al.* Graphite phase carbon nitride based membrane for selective permeation. *Nature Communications* 2019, **10**(1): 2500.
15. Ma X, Kumar P, Mittal N, Khlyustova A, Daoutidis P, Mkhoyan KA, *et al.* Zeolitic imidazolate framework membranes made by ligand-induced permselectivation. *Science* 2018, **361**(6406): 1008–

1011.

16. Jin X, Foller T, Wen X, Ghasemian MB, Wang F, Zhang M, *et al.* Effective Separation of CO2 Using Metal-Incorporated rGO Membranes. *Adv Mater* 2020, **32**(17): 1907580.
17. Zhao J, Zhao X, Jiang Z, Li Z, Fan X, Zhu J, *et al.* Biomimetic and bioinspired membranes: Preparation and application. *Progress in Polymer Science* 2014, **39**(9): 1668–1720.
18. Agre P. Aquaporin Water Channels (Nobel Lecture). *Angewandte Chemie International Edition* 2004, **43**(33): 4278–4290.
19. Nicolson GL. The Fluid—Mosaic Model of Membrane Structure: Still relevant to understanding the structure, function and dynamics of biological membranes after more than 40 years. *Biochimica et Biophysica Acta (BBA) - Biomembranes* 2014, **1838**(6): 1451–1466.
20. Ballweg S, Sezgin E, Doktorova M, Covino R, Reinhard J, Wunnicke D, *et al.* Regulation of lipid saturation without sensing membrane fluidity. *Nature Communications* 2020, **11**(1): 756.
21. Park G, Gabbaï FP. Phosphonium Boranes for the Selective Transport of Fluoride Anions across Artificial Phospholipid Membranes. *Angewandte Chemie International Edition* 2020, **59**(13): 5298–5302.
22. Shen F-F, Dai S-Y, Wong N-K, Deng S, Wong AS-T, Yang D. Mediating K+/H + Transport on Organelle Membranes to Selectively Eradicate Cancer Stem Cells with a Small Molecule. *J Am Chem Soc* 2020, **142**(24): 10769–10779.
23. Radha B, Esfandiar A, Wang FC, Rooney AP, Gopinadhan K, Keerthi A, *et al.* Molecular transport through capillaries made with atomic-scale precision. *Nature* 2016, **538**(7624): 222–225.
24. Shen Y-x, Song W, Barden DR, Ren T, Lang C, Feroz H, *et al.* Achieving high permeability and enhanced selectivity for Angstrom-scale separations using artificial water channel membranes. *Nature Communications* 2018, **9**(1): 2294.
25. Shen J, Ye R, Romanies A, Roy A, Chen F, Ren C, *et al.* Aquafoldmer-Based Aquaporin-like Synthetic Water Channel. *J Am Chem Soc* 2020, **142**(22): 10050–10058.
26. Wang S, Wu Y, Zhang N, He G, Xin Q, Wu X, *et al.* A highly permeable graphene oxide membrane with fast and selective transport nanochannels for efficient carbon capture. *Energy & Environmental Science* 2016, **9**(10): 3107–3112.
27. Song W, Joshi H, Chowdhury R, Najem JS, Shen Y-x, Lang C, *et al.* Artificial water channels enable fast and selective water permeation through water-wire networks. *Nature Nanotechnology* 2020, **15**(1): 73–79.
28. Song W, Lang C, Shen Y-x, Kumar M. Design Considerations for Artificial Water Channel–Based Membranes. *Annual Review of Materials Research* 2018, **48**(1): 57–82.
29. Lee CS, Choi M-k, Hwang YY, Kim H, Kim MK, Lee YJ. Facilitated Water Transport through Graphene Oxide Membranes Functionalized with Aquaporin-Mimicking Peptides. *Adv Mater* 2018, **30**(14): 1705944.

30. Kumar M, Habel JEO, Shen Y-x, Meier WP, Walz T. High-Density Reconstitution of Functional Water Channels into Vesicular and Planar Block Copolymer Membranes. *J Am Chem Soc* 2012, **134**(45): 18631–18637.
31. Tunuguntla RH, Henley RY, Yao Y-C, Pham TA, Wanunu M, Noy A. Enhanced water permeability and tunable ion selectivity in subnanometer carbon nanotube porins. *Science* 2017, **357**(6353): 792–796.
32. Geng J, Kim K, Zhang J, Escalada A, Tunuguntla R, Comolli LR, *et al.* Stochastic transport through carbon nanotubes in lipid bilayers and live cell membranes. *Nature* 2014, **514**(7524): 612–615.
33. Debnath M, Chakraborty S, Kumar YP, Chaudhuri R, Jana B, Dash J. Ionophore constructed from non-covalent assembly of a G-quadruplex and liponucleoside transports K+-ion across biological membranes. *Nature Communications* 2020, **11**(1): 469.
34. Schneider S, Licsandru E-D, Kocsis I, Gilles A, Dumitru F, Moulin E, *et al.* Columnar Self-Assemblies of Triarylamines as Scaffolds for Artificial Biomimetic Channels for Ion and for Water Transport. *J Am Chem Soc* 2017, **139**(10): 3721–3727.
35. Tu Y-M, Song W, Ren T, Shen Y-x, Chowdhury R, Rajapaksha P, *et al.* Rapid fabrication of precise high-throughput filters from membrane protein nanosheets. *Nat Mater* 2020, **19**(3): 347–354.
36. Hayes R, Imberti S, Warr GG, Atkin R. Amphiphilicity determines nanostructure in protic ionic liquids. *Physical Chemistry Chemical Physics* 2011, **13**(8): 3237–3247.
37. Hayes R, Warr GG, Atkin R. Structure and Nanostructure in Ionic Liquids. *Chemical Reviews* 2015, **115**(13): 6357–6426.
38. Hayes R, Imberti S, Warr GG, Atkin R. Effect of Cation Alkyl Chain Length and Anion Type on Protic Ionic Liquid Nanostructure. *The Journal of Physical Chemistry C* 2014, **118**(25): 13998–14008.
39. Goossens K, Lava K, Bielawski CW, Binnemans K. Ionic Liquid Crystals: Versatile Materials. *Chemical Reviews* 2016, **116**(8): 4643–4807.
40. Mao X, Brown P, Červinka C, Hazell G, Li H, Ren Y, *et al.* Self-assembled nanostructures in ionic liquids facilitate charge storage at electrified interfaces. *Nat Mater* 2019, **18**(12): 1350–1357.
41. Mendonça CMN, Balogh DT, Barbosa SC, Sintra TE, Ventura SPM, Martins LFG, *et al.* Understanding the interactions of imidazolium-based ionic liquids with cell membrane models. *Physical Chemistry Chemical Physics* 2018, **20**(47): 29764–29777.
42. Dou H, Jiang B, Xu M, Zhang Z, Wen G, Peng F, *et al.* Boron Nitride Membranes with a Distinct Nanoconfinement Effect for Efficient Ethylene/Ethane Separation. *Angew Chem Int Ed* 2019, **131**(39): 14107–14113.
43. Ghysels A, Krämer A, Venable RM, Teague WE, Lyman E, Gawrisch K, *et al.* Permeability of membranes in the liquid ordered and liquid disordered phases. *Nature Communications* 2019, **10**(1): 5616.
44. Lin R-B, Li L, Zhou H-L, Wu H, He C, Li S, *et al.* Molecular sieving of ethylene from ethane using a rigid metal–organic framework. *Nat Mater* 2018, **17**(12): 1128–1133.

45. Li L, Lin R-B, Krishna R, Li H, Xiang S, Wu H, *et al.* Ethane/ethylene separation in a metal-organic framework with iron-peroxo sites. *Science* 2018, **362**(6413): 443–446.
46. Jiang B, Zhou J, Xu M, Dou H, Zhang H, Yang N, *et al.* Multifunctional ternary deep eutectic solvent-based membranes for the cost-effective ethylene/ethane separation. *J Membr Sci* 2020: 118243.
47. Dou H, Jiang B, Zhang L, Xu M, Sun Y. Synergy of high permeability, selectivity and good stability properties of silver-decorated deep eutectic solvent based facilitated transport membranes for efficient ethylene/ethane separation. *J Membr Sci* 2018, **567**: 39–48.
48. Zhang Z, Luo D, Li G, Gao R, Li M, Li S, *et al.* Tantalum-Based Electrocatalyst for Polysulfide Catalysis and Retention for High-Performance Lithium-Sulfur Batteries. *Matter* 2020.
49. Wen G, Ren B, Park MG, Yang J, Dou H, Zhang Z, *et al.* Ternary Sn-Ti-O Electrocatalyst Boosts the Stability and Energy Efficiency of CO2 Reduction. *Angewandte Chemie International Edition* 2020, **n**/**a**(n/a).
50. Jiang B, Dou H, Wang B, Sun Y, Huang Z, Bi H, *et al.* Silver-Based Deep Eutectic Solvents as Separation Media: Supported Liquid Membranes for Facilitated Olefin Transport. *ACS Sustain Chem, Eng* 2017, **5**(8): 6873–6882.
51. Jiang B, Dou H, Zhang L, Wang B, Sun Y, Yang H, *et al.* Novel supported liquid membranes based on deep eutectic solvents for olefin-paraffin separation via facilitated transport. *J Membr Sci* 2017, **536**: 123–132.
52. Dou H, Jiang B, Xiao X, Xu M, Wang B, Hao L, *et al.* Ultra-stable and cost-efficient protic ionic liquid based facilitated transport membranes for highly selective olefin/paraffin separation. *J Membr Sci* 2018, **557**: 76–86.
53. Dou H, Jiang B, Xiao X, Xu M, Tantai X, Wang B, *et al.* Novel Protic Ionic Liquid Composite Membranes with Fast and Selective Gas Transport Nanochannels for Ethylene/Ethane Separation. *ACS Appl Mater Inter* 2018, **10**(16): 13963–13974.

Figures

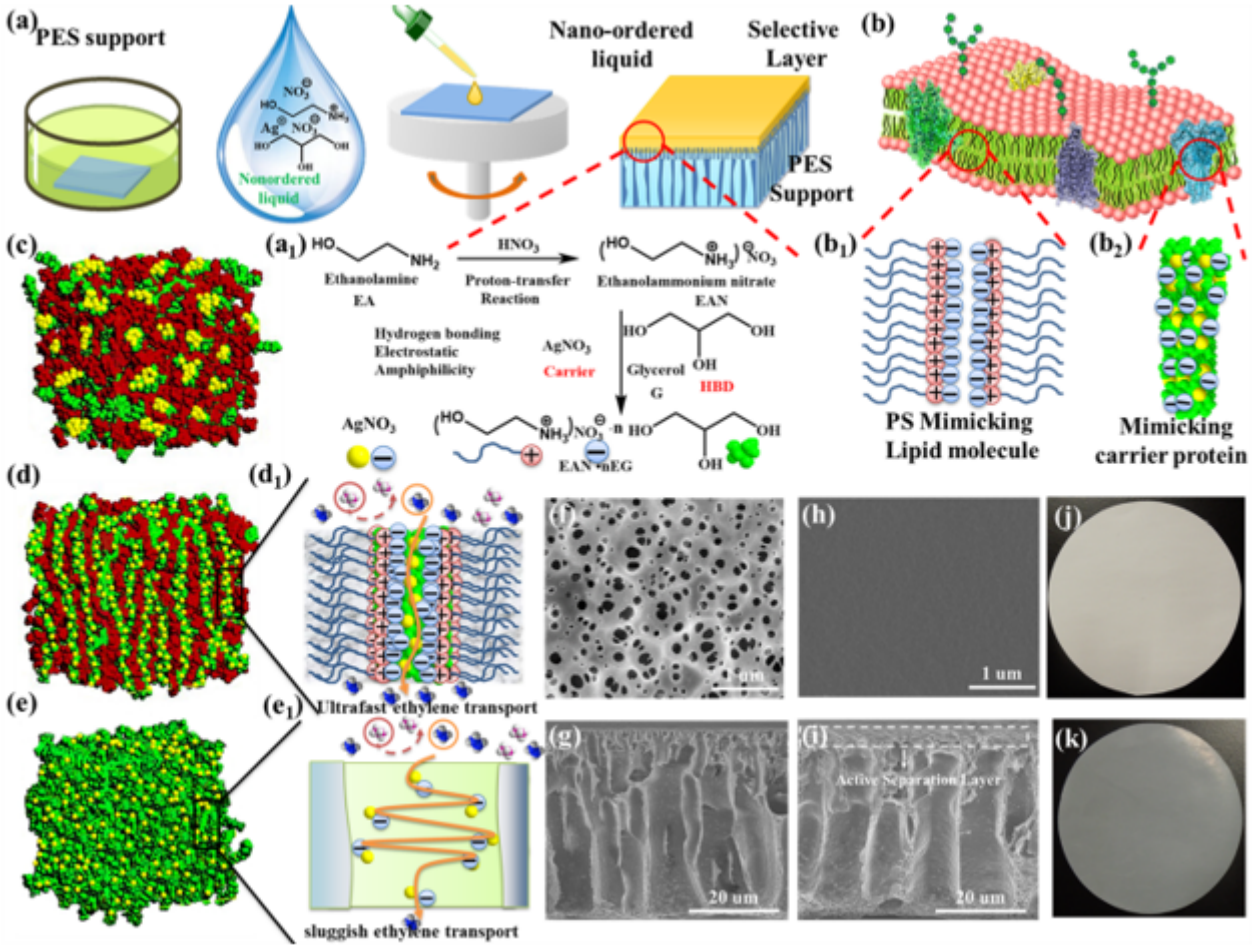

Figure 1

Design of bioinspired nano-ordered liquid membrane and their morphology characterization. (a) The fabrication of bioinspired nano-ordered liquid membrane: preparation of PES support, synthesis of bioinspired nano-ordered liquid, construction of membrane by spin-coating, (a1) synthetic route of nano-ordered liquid. (b) Structure of cellular membranes with transmembrane proteins embedded in the phospholipid bilayer: (b1) the self-assembly of PSs mimicking the lipid bilayer, (b2) the self-assembly of glycerol embedded within carrier mimicking the carrier protein. (c) Structure of bioinspired nano-ordered liquid membrane with lousily carrier aggregation. (d, d1) Structure of bioinspired nano-ordered liquid membrane with enormous 3D interconnected ethylene transport nanochannels, and the correspondingly highlighted nanochannel. (e, e1) Structure of traditional polymer or liquid membrane with random carrier distribution and the highlighted sluggish ethylene transport. (f-g) SEM images of top and cross-section of homemade PES support. (h, i) SEM images of top and cross-section of bioinspired nano-ordered liquid membrane. (j, k) Photos of PES support and bioinspired nano-ordered liquid membrane.

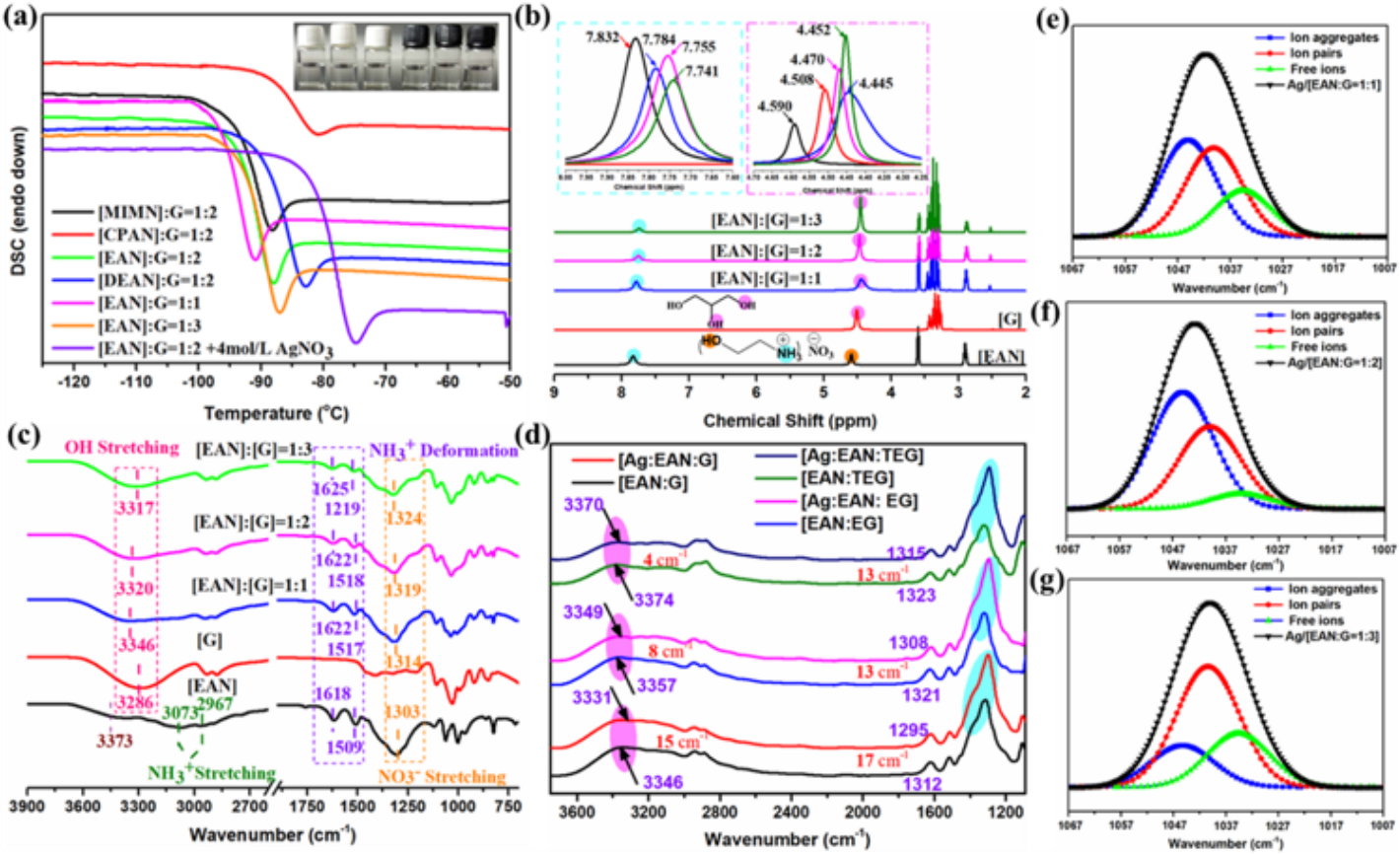

Figure 2

The intermolecular interactions for self-assembly and structure of bioinspired nano-ordered liquid membranes. (a) Binary eutectics of PSs and polyols, and ternary eutectics of PSs, polyols and carrier. (b. c) Demonstrations of hydrogen bonding and electrostatic attractions between PSs and polyols by 1HNMR (b) and ATR-FTIR spectra (c). (d) Investigation the interactions between carrier and PSs or polyols by ATR-FTIR spectra. (e, f and g) Elucidate of existent forms of NO3- anions and the according contents within membranes at the molar ratios of 1:1, 1:2 and 1:3 by FT-Raman spectra.

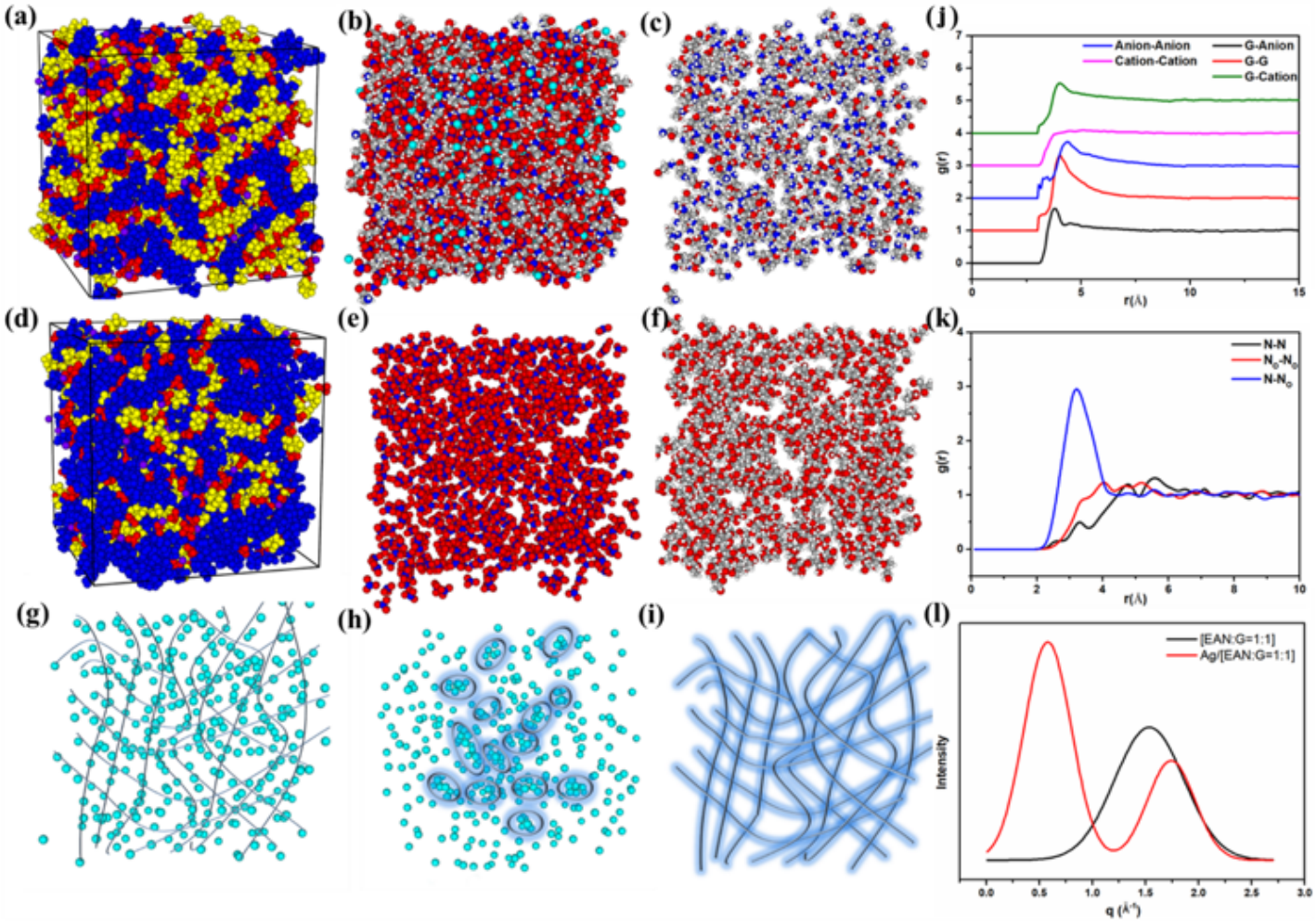

Figure 3

The regular carrier wires and formation of enormous 3D interconnected ethylene transport nanochannels. (a) Highlighted snapshot bulk structure of bioinspired nano-ordered liquid membrane (EAN: glycerol = 1:1) with the yellow EAN cations, red anions and blue G molecules. (b, c, e and f) Snapshots of molecular simulations of bioinspired nano-ordered liquid membrane, where the carbon, hydrogen, oxygen, nitrogen and silver atoms are shown in in grey, in white, in red, in blue and in Tiffany blue, respectively, (b) all atoms, (c) EAN cations, (e) NO3- anions of EAN and silver salt (f) G molecules. (d) Highlighted snapshot bulk structure of bioinspired nano-ordered liquid membrane (EAN: glycerol = 1:2) with the yellow EAN cations, red anions and blue G molecules. (g, h) Distribution of silver cations within bioinspired liquid membranes with EAN/G molar ratios of 1:1 or 1:2. (i) Highlighted carrier wires. (j) Radial distribution functions of the centers of masses of ion-ion or ion-molecular. (k) Radial distribution functions of N atom-N atom of cation-anion of EAN; (l) SWAXS patterns of bioinspired nano-ordered liquid membrane.

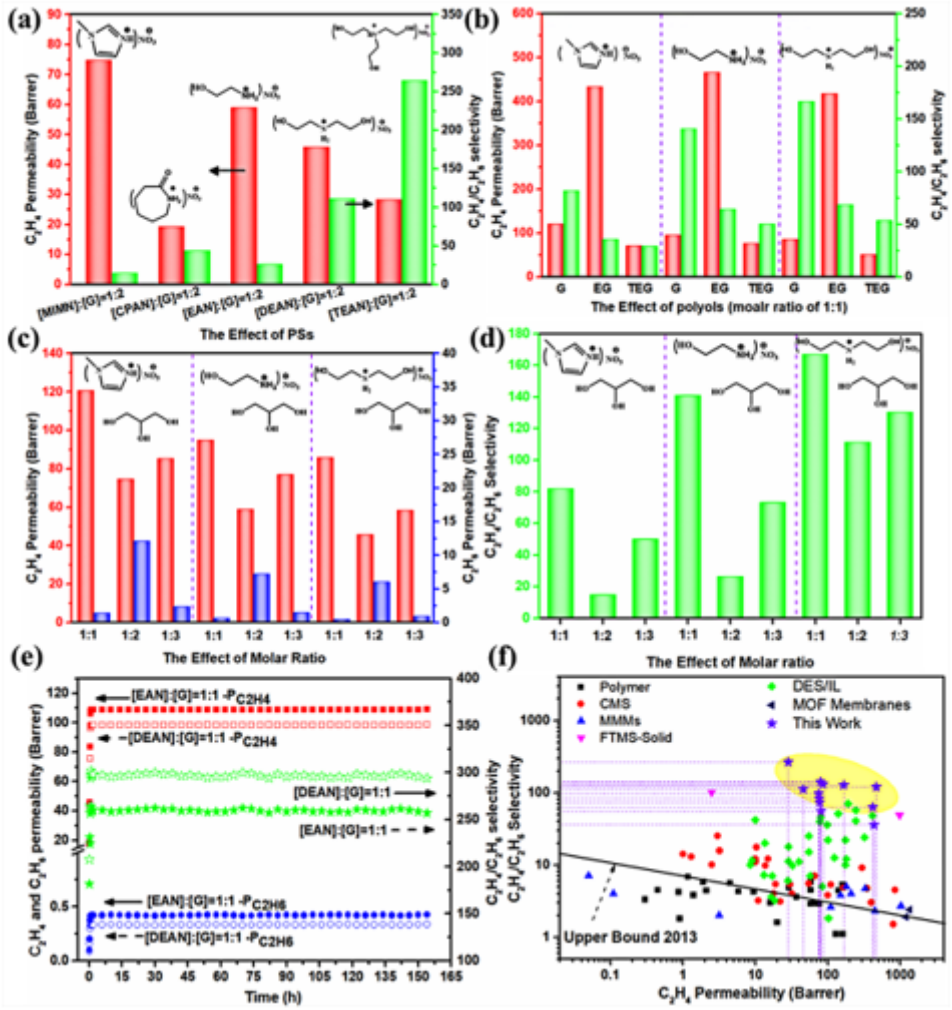

Figure 4

The structure-performance relationship and corresponding performances of bioinspired nano-ordered liquid membranes for precise ethylene/ethane separation. (a) Effect of PSs on separation performance. (b) Effect of polyols on separation performance. (c) Effect of molar ratio on the gas permeability. (d) Effect of molar ratio on the selectivity. (e) Evaluation of the long-term stability of bioinspired nano-ordered liquid membranes. (f) Comparison of bioinspired nano-ordered liquid membranes with the state of art of membranes for ethylene/ethane separations, where the data are plotted on a log-log scale.

Supplementary Files

This is a list of supplementary files associated with this preprint. Click to download.

- SupportinginformationHZ.docx